Comparison of the solid oxide fuel cell system for micro CHP using natural gas with a system using a mixture of natural gas and hydrogen

Cinti, G.; Bidini, G.; Hemmes, K.

DOI
10.1016/j.apenergy.2019.01.039

Publication date
2019

Document Version
Accepted author manuscript

Published in
Applied Energy

Citation (APA)
Cinti, G., Bidini, G., & Hemmes, K. (2019). Comparison of the solid oxide fuel cell system for micro CHP using natural gas with a system using a mixture of natural gas and hydrogen. *Applied Energy*, *238*, 69-77. https://doi.org/10.1016/j.apenergy.2019.01.039

Comparison of the solid oxide fuel cell system for micro CHP using natural gas with a system using a mixture of natural gas and hydrogen

G. Cinti[a, *]
giovanni.cinti@unipg.it

G. Bidini[a]

K. Hemmes[b]

[a]Università degli Studi di Perugia, Dipartimento di Ingegneria, via Duranti 93, Perugia, Italy

[b]TU Delft, Faculty of Technology, Policy and Management, Jaffalaan 5, 2628 BX Delft, the Netherlands

[*]Corresponding author.

Abstract
Solid oxide fuel cell systems for combined heat and power production (SOFC μCHP) fuelled by natural gas are attractive because of their high electrical and total efficiency even at small scale. The development of a hydrogen economy will increase the availability of distributed hydrogen as a pure gas. Alternatively, hydrogen may be blended with natural gas in the grid. This study investigates the performance of SOFC μCHP systems, while using a fuel varying from pure hydrogen to pure methane via mixtures of hydrogen and methane called Hythane. Flowsheet models of external as well as internal reforming fuel cell systems were developed in Cycle-Tempo simulation software. Results show that both the external as well as the internal reforming system can operated on all fuel gas compositions varying from pure hydrogen to pure methane, thus allowing for a transition towards a hydrogen economy via the mixing of hydrogen into the natural gas grid. Although the natural gas based systems have a higher electrical efficiency, the introduction of hydrogen into the gas leads to a higher total efficiency of the combined heat and power system. The addition of hydrogen into the fuel minimizes the problems of thermal stress and thermal shock associated with the use of methane in internal reforming fuel cell systems. The internal reforming system showed a higher performance compared to the external reforming system for all Hythane gas mixtures in terms of not only electrical efficiency but also in terms of thermal and total efficiency.

Keywords: SOFC; μCHP; Hythane; Distributed generation

Nomenclature
(μ)CHP
(micro) combined heat and power

RES
renewable energy sources

SOFC
solid oxide fuel cell

OCV
open circuit voltage

ER
external reforming

IR
internal reforming

AB
after burner

HE
heat exchanger

ASR
area specific resistance

Uf

fuel utilization in the SOFC

Uox
oxygen utilization in the SOFC

S2C
steam to carbon ratio

LHV
lower heating value

HHV
higher heating value

1 Introduction

One of the ways to lower CO_2 emissions is a transition towards a hydrogen economy. One of the main obstacles for the development of hydrogen as an energy carrier is the cost of the development of a hydrogen distribution infrastructure. To avoid this obstacle several studies proposed to take advantage of the existing wide spread natural gas grid. Hydrogen can be mixed with methane in the present pipelines. The mixture of hydrogen and methane is sometimes called Hythane. In order to accelerate the transition towards a hydrogen economy the introduction of hydrogen into the natural gas grid is studied in several projects and reported in literature [1–6]. Van de Beld et al. showed that it is not just about the mixing of hydrogen into the natural gas grid, but that also specific production methods can be developed for producing the mixture directly. This has several advantages compared to the production of pure components first and later mixing them [1]. In a large EU project called NATURALHY the blending of hydrogen into natural gas has been extensively studied from many different perspectives [2]. The allowable percentages of hydrogen that can be mixed into a natural gas system has been studied specifically by Altfeld and Pinchbeck [3]. Lewinsky et al. focussed on the impact of natural gas/hydrogen mixtures on the performance of end-use equipment and domestic appliances [4], while Guandalini et al. [5] focussed on the consequences for the high pressure transport pipelines and Abeysekera et al. [6] studied the network as a whole under distributed injection of hydrogen containing gas mixtures.

A system operating with Hythane instead of natural gas can reduce overall CO_2 emissions due to the use of hydrogen produced from renewable energy sources (RES). Moreover, we propose, in this study, the use of fuel cell technology, that is well known for its quasi zero emission in terms of pollutants.

Hythane can be used in all applications of methane in the residential field (heating, cooking), in the stationary power generation field, such as cogeneration and power production, and in the transport sector where natural gas fueled vehicles can also be operated on Hythane with significant advantages in terms of emission reductions [7–10]. In other words, Hythane can substitute methane in many of the applications where combustion occurs with the advantage of reduced CO_2 emissions due to the contribution of hydrogen. Compared to a pure hydrogen system, power units operating on Hythane are limited in terms of sustainability because the fuel still contains carbon that is most likely but not necessarily fossil based. The share of renewable energy can be increased somewhat further if the methane used in the grid comes from biomass treatment (e.g. upgraded biogas from anaerobic digestion) [11–14], from renewable electricity (power to gas) [15–17] or a combination of both [18].

In our vision three potential paths for the introduction of Hythane into our energy system can be envisioned:

–

A blend of hydrogen and natural gas available in the present natural gas grid. Such a scenario is strongly dependent on the evolution of a hydrogen economy. A huge amount of hydrogen is required to increase the hydrogen concentration in the grid even if only up to a few percent. Such a scenario may develop if power to gas technology with hydrogen, as a storage option for renewable electricity, will strongly increase. Or if carbon capture and storage will be applied on a large scale in the production of hydrogen for the natural gas grid from fossil fuel resources such as from natural gas itself. Due to the extra cost it is obvious that strong incentives, such as a high carbon tax should be in place. In addition several studies reported in literature [4,19,20] and a FP6 EU project called Naturalhy [2] investigated the tolerance limits of the natural gas grid for hydrogen addition. Levinsky et al. assessed that the safety limit for the maximum amount of hydrogen to be mixed into natural gas depends on the composition of the natural gas [4]. A, maximum value

of 10 vol% of hydrogen is generally considered, due to safe combustion limits in end user appliances[5]. Still even this maximum of 10 vol% of hydrogen is only 3% in terms of energy content. If we consider a future scenario where the use of combustion based technologies will be strongly reduced and the burners in remaining appliances adapted, such a limit can move up to 50 vol% and above.

–

An interesting second option comes from processes that avoid the production of pure hydrogen and instead directly yield Hythane as output. Such technologies can be based on natural gas or biomass methane and encompasses conversion technologies such as steam methane reforming with low CH_4 conversion, incomplete plasma or thermal decomposition of methane and possibly internal reforming fuel cells as well. Incomplete thermal decomposition of natural gas has, for example, been studied in conjunction with concentrated solar energy by the authors of this paper [21]. We have proposed large-scale thermal decomposition of natural gas in the North of Africa while transporting the directly produced Hythane through existing natural gas pipelines to Europe. In this option, we would not be talking about mixing hydrogen into the natural gas but rather look at it as taking the carbon out. When taking biomass as the fuel both bio-reactors using bacteria and super critical gasifiers can produce a blend of methane and hydrogen with inherent advantages in the process itself compared to pure hydrogen production. Advantages and opportunities of such paths are reported in literature [1].

–

As a third option the gas blend can be obtained at a local level by mixing natural gas from the grid with hydrogen locally produced from renewable energy sources. Natural gas might be used to support hydrogen energy supply when the energy from Renewable energy sources (RES) stored in the form of hydrogen is not sufficient to feed the system and fulfill the demand. Strategies can be elaborated to take maximum advantage of the use of hydrogen from RES and natural gas from the grid.

In parallel with new concepts such as Hythane, a development towards distributed generation can be observed for electricity as well as for the gas sector [22]. In particular, the distributed production of electricity in combination with the development of smart grids supported the development of small power cogeneration plants connected to the natural gas grid as well as the electricity grid while waste heat is used locally. In this cogeneration or combined heat and power application, fuel cells and, especially, high temperature fuel cells such as Solid Oxide Fuel Cells (SOFC), can achieve the highest energy efficiencies in terms of power production compared to competitive technologies [23]. The market opportunity for micro cogeneration of heat and power (μCHP) application on the scale of a household or group of houses, brought several SOFC producers and system developers to start demonstrating this technology mainly in Europe [24–26] and in Japan [27,28]. Recent research focuses on the optimization of system design [29–35] and the study of μCHP integration strategies [36–40]. System design studies have been performed applying external reforming [29,31,33], innovative designs with low temperature SOFC's [32], with and without gas recirculation [30] and substitution of steam reforming by dry reforming [34,35]. The integration strategy studies focus mainly on the economical valorization of heat and power depending on the specific geographical application conditions [36], on the type of building [37,38] and on the network integration strategy [39]. Recently also the integration of SOFC systems fed with biogas at an industrial scale was studied [40].

Simultaneous technology developments can reinforce each other or can have a negative influence on the diffusion of one or both of the technologies. Up to our knowledge the interaction between the developments sketched above and the possible consequences for SOFC operation and development have not been studied. Therefor the aim of this study in particular is to evaluate the performance of a μCHP system based on SOFC technology when fed with Hythane compared to standard operation using methane (natural gas). This study starts from the idea of placing an existing (semi-)commercial μCHP unit based on the SOFC in a future scenario where Hythane will feed the system. No modification nor optimization of this SOFC system design is considered. The research questions we would like to answer are:

1.

What would be the efficiency of the system operating on a mixture of hydrogen and natural gas compared to the same system running on pure natural gas? Would it increase or would it decrease due to the addition of hydrogen?

2.

Irrespective of the efficiency would there be other advantages or disadvantages running the system on a mixture of natural gas and hydrogen?

3.

Would it make a difference if the SOFC system was based on an internal reforming SOFC or if external reforming was applied in the cogeneration system?

2 System design

By mixing hydrogen into the natural gas, we expect the Nernst potential to increase due to the higher hydrogen partial pressure in the mixture. A higher Nernst potential or open circuit voltage (OCV) in general means a higher efficiency. On the other hand, the reforming of natural gas is an endothermic reaction taking away a lot of the waste heat produced in the fuel cell thereby upgrading the waste heat into chemical energy again, which makes, in particular, internal reforming fuel cells so very attractive from a thermodynamic point of view. Moreover, a higher Nernst potential often also induces a higher Nernst loss in the fuel cell because, on average, the Nernst potential is still comparable with the situation in which less hydrogen would be introduced in the fuel yielding more or less the same averaged Nernst potential over the whole cell, making the average deviation (by definition, the Nernst loss) with the higher OCV larger. Therefore, in our simulations we must be careful to include Nernst loss in a proper way and not simply model the fuel cell with an internal resistance or just with a fixed polarization. The flow sheet program we are using is called Cycle-Tempo and has this calculation of the Nernst loss in the fuel cell module in the correct way. The flow sheet program Cycle-Tempo is described elsewhere and is used in many studies of energy systems [41] and also in many fuel cell energy systems studies [21,42,43].

A cogeneration system based on SOFCs is usually composed of the SOFC stack, the fuel processing unit with external reformer, the air flow management, off gasses treatment and the thermal control network. Fuel processing in the reformer allows to obtain a hydrogen rich mixture from the supplied fuel and to reach the SOFC inlet temperature. As is well known, steam reforming of methane is endothermic so next to methane and steam also heat has to be supplied. This is accomplished by connecting the reformer to the outlet of the after-burner. Air flow management ensures the supply of the required amount of preheated air to the cathode. Usually excess air is supplied to cool the SOFC. Anode off-gas treatment is generally realized by using an after- burner that completes the oxidation of unreacted fuel. Finally, in order to provide proper heat recovery and effective heat integration the system design is complemented by heat exchangers, mixers and gas stream dividers.

The scheme of the SOFC system under study is shown in Fig. 1 and was modeled using Cycle Tempo. The design is derived from an online standard model that can be downloaded from Cycle Tempo website [44]. The system integrates a SOFC stack, an external reforming unit (ER) and an after burner (AB). It represents a typical design of an intermediate temperature SOFC system (750 °C). In detail, the complete oxidation of anode off-gas is achieved in the after burner (AB) where the fuel gas flow is mixed with the cathode outlet. The off gasses of the cathode have more oxygen than required for the after burner since there always is an excess cathode air flow to cool down the stack. Thus, a gas flow divider (S1) is added to supply only a limited amount of oxidant flow to the burner to obtain the right design temperature of the AB exhausts. After burner off gasses flow through the reformer (ER) and a heat exchanger (HE1) that pre-heats the inlet fuel up to mixer M1, where steam and fuel are premixed before entering the reformer. In the mixer M2, the AB off gasses are mixed with the other part of the cathodic off-gas that is separated in S1. Before reaching M2, this cathodic stream preheats the cathode inlet gas in the high temperature heat exchanger HE2 up to stack inlet temperature. M2 gas outlets reach heat exchanger HE3 that provides intermediate preheating of the air inlet flow. The residual heat in the gas flow is then split in S2. Part of the S2 outlet reaches HE6 where low temperature heating is performed from room temperature while the rest of the gas from S2 is required to heat up the water stream in three different stages: economizer (HE7), evaporator (HE5) and superheater (HE4). The two streams separated in S2 are mixed back in mixer M3 before reaching the cogeneration unit (CH) and vented finally into atmosphere via the blower B. Heat extracted in CH is the thermal output of the system. Table 1 reports the design temperatures used in this study. Thermal equilibrium of the stack is defined by the gas inlet (700 °C) and outlet (800 °C) temperature. Thermal equilibrium of the SOFC is obtained by the model by controlling the air inlet gas flow. Thermal equilibrium of the reformer is obtained by recovering more or less heat from the afterburner (AB) exhaust gas stream. In the modelling of the reformer unit, chemical equilibrium of all reformer reactions is assumed at the outlet temperature. Both fuel and steam inlet flows are designed to be at 400 °C and the syngas outlet is set at the same temperature as the SOFC inlet: 700 °C. Pressure drops of 20 mbar were considered for all heat exchangers, the reformer and in the after

burner. Regarding the SOFC stack, pressure losses of 20 mbar are implemented at the anode and 50 mbar at the cathode.

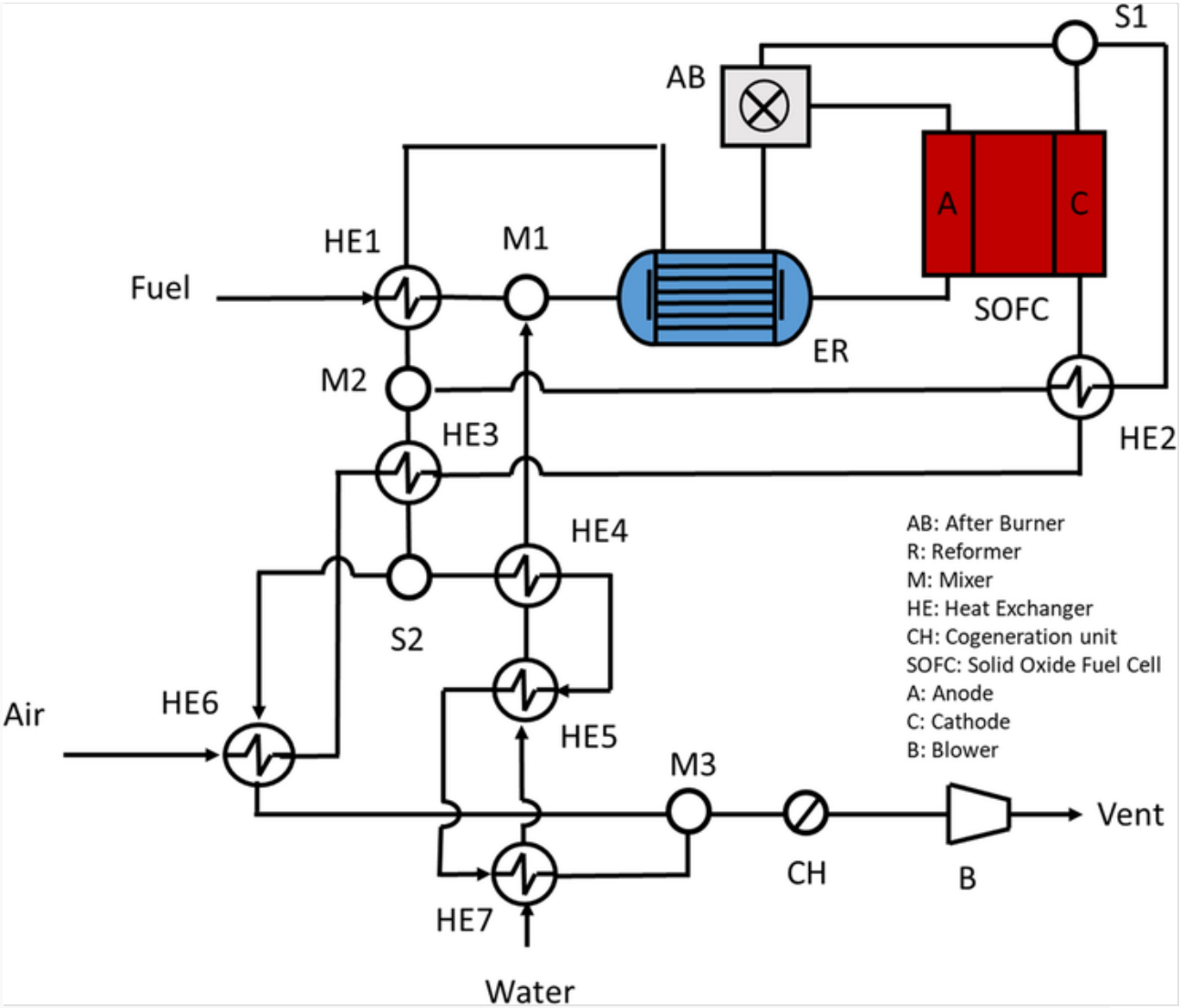

Fig. 1 Scheme of the SOFC CHP system design.

Table 1 Design specifics of the system.

SOFC stack temperature (°C)	750
SOFC stack inlet temperature (°C)	700
SOFC stack outlet temperature (°C)	800
Reformer reaction temperature (°C)	700
Burner outlet temperature (°C)	1200
Reformer gas inlet temperature (°C)	400

Reformer gas outlet temperature (°C)	700
HE6 air outlet temperature (°C)	350
HE7 water outlet temperature (°C)	99
HE5 steam outlet temperature (°C)	101
HE4 steam outlet temperature (°C)	400
Pressure losses in Heat exchangers (bar)	0.02

In the internal reforming based system, the reformer is substituted by a heat exchanger and the cell was operated in internal reforming mode. System design temperature and pressure losses are reported in Table 1.

The SOFC input design parameters, in addition to the temperatures defined in Table 1 are: total active area, area specific resistance (ASR) and fuel utilization (U_f). The model calculates utilization of oxygen (Uox) from the air flow and current density. ASR is the slope of the voltage versus current density curve. For this study the ASR value was obtained from commercial SOLiDPower ASC700 cells that, at 750 °C have a value of $2.8 \cdot 10^{-5}\ \Omega\ m^2$ [45]. The gas utilization Uf and Uox parameters are defined as follows:

$$U_f = \frac{N \cdot I}{2 \cdot F \cdot n_{H2}} \quad \text{(i)}$$

$$U_{ox} = \frac{N \cdot I}{4 \cdot F \cdot n_{O2}} \quad \text{(iii)}$$

In the equations N is the number of cells, I is cell current, F is Faraday's constant an n_{H2} and n_{O2} are hydrogen and oxygen molar flow respectively.

Air flow is obtained from stack thermal equilibrium as to maintain the design output temperatures. The reformer is designed to operate at a constant reaction equilibrium temperature of 700 °C and a steam to carbon ratio of 2.2. The same steam to carbon ratio was maintained for both internal as well as external reforming system operation.

Note that the model is designed to evaluate the system performances once changing the gas mixture inlet composition. In this sense, the model simulates the performances of a system designed for natural gas application that operates with the new blends. Thus, the analysis was performed by keeping the stack design parameters such as active area and internal resistance constant. Also fuel utilization and stack power were kept constant during the simulation. In detail, a DC stack power output of 1.25 kW was imposed in the model. Thereby a net system power in the range of 1 kW is obtained. We assume that components such as reformer, heat exchangers and burner can operate with the new gas flow composition under otherwise the same conditions. SOFC stack design parameters are reported in Table 2.

Table 2 SOFC stack input data.

Total active area – m^2	300
Area specific resistance (ASR) – $\Omega\ m^2$	$2.8 \cdot 10^{-5}$
Utilization of fuel	0.8

Power output (DC) – W	1225
Anodic pressure losses – bar	0.02
Cathodic pressure losses – bar	0.05

The aim of this study is to evaluate the systems operating on pure methane with the same systems operating on Hythane, therefore the model was run with 6 different gas compositions from pure methane to 1% of CH_4 into hydrogen (the software does not allow 0% CH_4 nor 100% H2). Table 3 reports the six gas compositions used in the simulations.

Table 3 Gas composition and S/C ratio of inlet fuel used in the simulations.

#	CH_4:H_2	S2C
1	100:0	2.2
2	80:20	2.2
3	60:40	2.2
4	40:60	2.2
5	20:80	2.2
6	1:99	2.2

The introduction of hydrogen in the fuel mixture allows additional system considerations. Looking to methane as a fuel, one of the main operation limits is related to the risk of carbon deposition in pipes and in the reformer catalyst. Decreasing the concentration of carbon fuel in the input gas mixture eventually permits to bypass the pre-reactor and therefore permits the use of a direct internal reforming fuel cell configuration.

Gas mixtures can be plotted in a ternary diagram to predict the effect in terms of carbon deposition or re-oxidation of the catalyst (Fig. 2). All gas compositions used in this study are shown in Table 3.by adjusting the amount of added steam to the chosen CH_4/H_2 blends we have imposed a S2C ratio of 2.2 to all the gas compositions and therefore they all lie in the safe area in between carbon deposition and nickel oxidation.

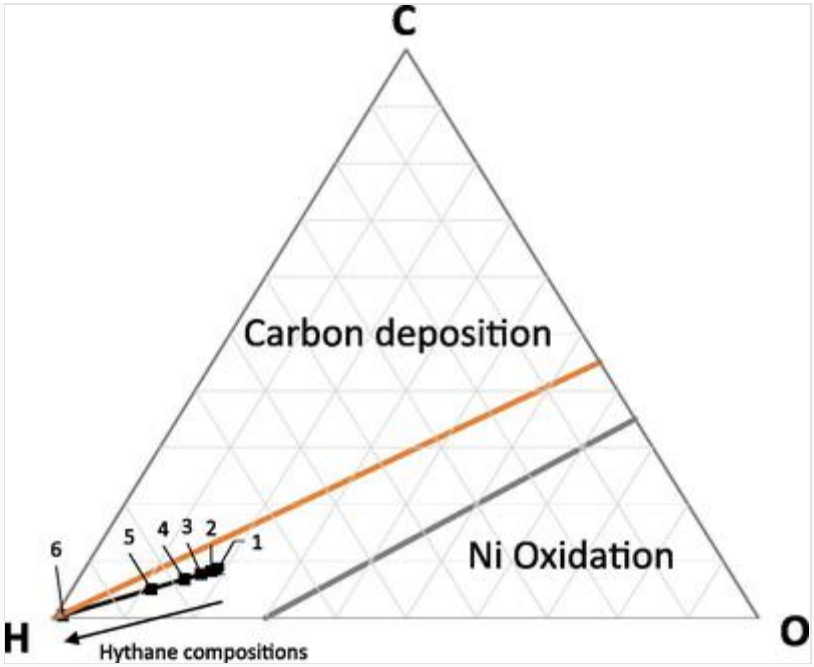

Fig. 2 Ternary HCO diagram of the selected compositions.

The fuel gas compositions used are reported in Fig. 2, and are acceptable for the catalyst in the reformer and in the cell. For internal reforming configurations the addition of hydrogen to the fuel may improve the reaction equilibrium and the electrochemical reaction kinetics and reduce the potential of thermal shocks that is the main drawback of internal reforming designs.

In conclusion two SOFC cogeneration system configurations were simulated; one with external reforming (ER) and one with an internal reforming (IR) SOFC using six fuel gas compositions.

3 Results

3.1 External reforming

For each simulation the gas composition was changed. Due to the imposed constant steam to carbon ratio of 2.2, a change of gas composition brings about an increase of water consumption for higher values of the CH_4 concentration. Reformer operation is strongly affected by the fuel gas composition in terms of thermal equilibrium and chemical products. Fig. 3(a) depicts the gas flows and relative chemical power supplied through the fuel inlet and anode inlet. Fuel inlet is the fuel mixture entering the system while anode inlet is the same as external reformer outlet i.e. the syngas mixture entering the fuel cell stack. The graph shows an increase of fuel inlet flow (mass based) when moving from Hythane to pure methane but at the same time a decrease in terms of energy flow. This opposite trend is caused by the different mass energy ratio of the different Hythane compositions. The decrease in terms of inlet power is caused by the varying system efficiency as will be discussed in the following. The anode inlet flow is higher than the fuel flow due to the introduction of steam, the concentration of which increases with an increase in methane concentration. For pure hydrogen fuel, no steam is added in the reformer and the anode inlet flow is the same as the fuel inlet flow. Anode inlet power is nearly constant for all fuel gas mixtures. Even if the mass flow is higher, the heating value of the mixture is lower due to the diluting effect of adding steam. As a net result the chemical power entering the stack is nearly constant. Anodic inlet gas composition as a function of methane concentration in the fuel gas is shown in Fig. 3(b). As anticipated, the increase of methane content in the flow has a diluting effect due to the corresponding imposed increase of steam and the formation of more CO_2 in the reformer due to this addition of steam.

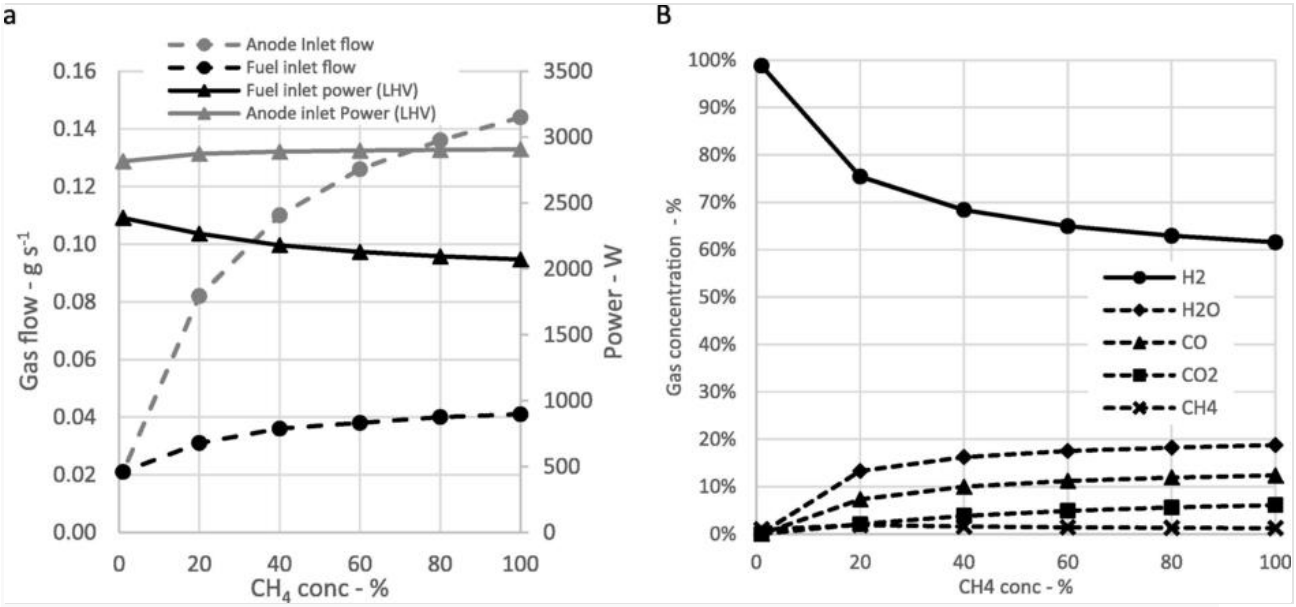

Fig. 3 (a) System fuel and anode inlet flue and (b) Anode inlet composition as function of CH_4 concentration in the Hythane.

Stack equilibrium is calculated at constant fuel utilization and constant electric output power. This results in a cell voltage and current density as a function of methane concentration in the fuel gas as shown in Fig. 4(a). The efficiency of the fuel cell stack is shown in Fig. 4(b). The cell voltage is higher when the system is operated with Hythane with a higher hydrogen content. As discussed in the introduction a higher hydrogen concentration results in a higher OCV and in general also in a higher cell voltage during operation. Vice versa, the current density has to decrease when cell voltage increases in order to fulfill the boundary condition of constant electric output power that we imposed on the system. A lower cell voltage of the SOFC obviously leads to a lower stack efficiency as shown in Fig. 4(b).

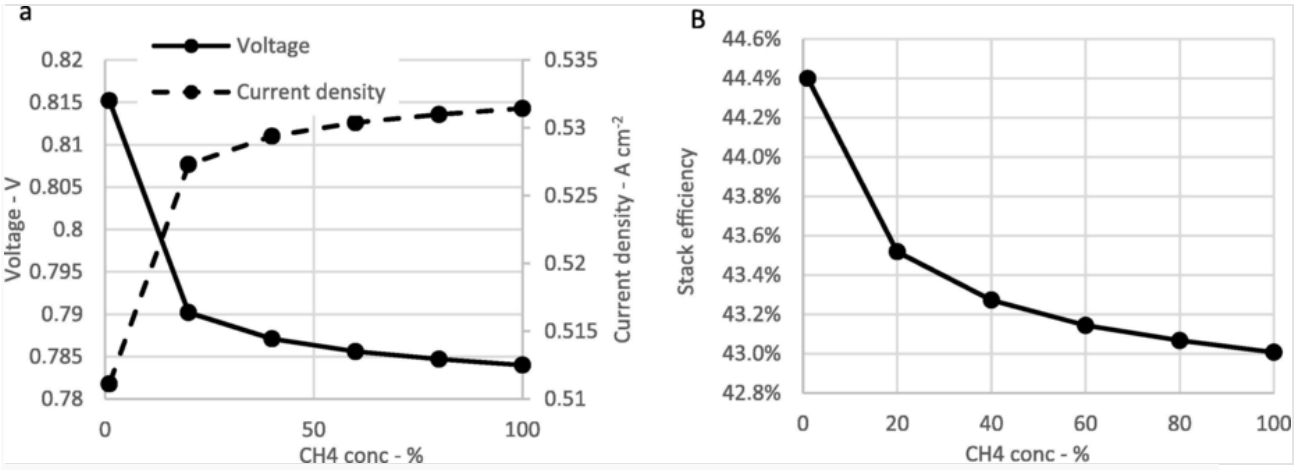

Fig. 4 SOFC performances in external reforming case. Voltage and current density Vs CH4 concentration (a) and efficiency Vs CH4 concentration (b).

Moving to system level, the introduction of hydrogen in the inlet gas brings two interesting results. Fig. 5(a) reports net, thermal and total efficiency at system level. When the system operates with pure methane, the electrical efficiency is found to be 48.44% and total efficiency is 75.07%, both based on LHV.

Such values are in line with the state of the art of the technology as reported in [46]. Efficiencies are calculated as heat, power and total energy output divided by the lower heating value (LHV) of the chemical energy in the input fuel flow in terms of energy per unit time (kW). Curves show a higher electrical efficiency of the system operating on pure methane compared to the same system operating on Hythane. On the other hand, when using Hythane higher thermal efficiencies and – in general - higher total efficiencies are obtained in the simulations. The lower electrical efficiency when using Hythane instead of methane is caused by a reduced contribution of the reformer to the system. The reformer reactor converts internally dissipated heat into chemical energy via the endothermic reforming reaction(s) in the reactor. This leads to higher hydrogen flows and increased chemical energy input into the stack and, therefore, via the imposed boundary condition of constant power output to a reduction of primary energy (fuel) input. When adding hydrogen into the gas mixture, the reduced heat absorption in the reactor results in a higher heat content in the off gasses and a higher heat production of the total system. This increase in thermal efficiency is also related yet for a smaller amount, to the larger higher heating value (HHV) of Hythane compared to methane. As stated, our efficiency calculations are based on the lower heating value but heat recovery our cogeneration system is performed down to 40 °C and therefore, condensation heat is included in the heat output but not accounted for in the input, following the most frequently used convention for condensing boilers. In general, as shown in Fig. 5(b), more chemical energy input is necessary as more hydrogen is introduced into the fuel under the boundary condition of constant electric power output as used in our simulations.

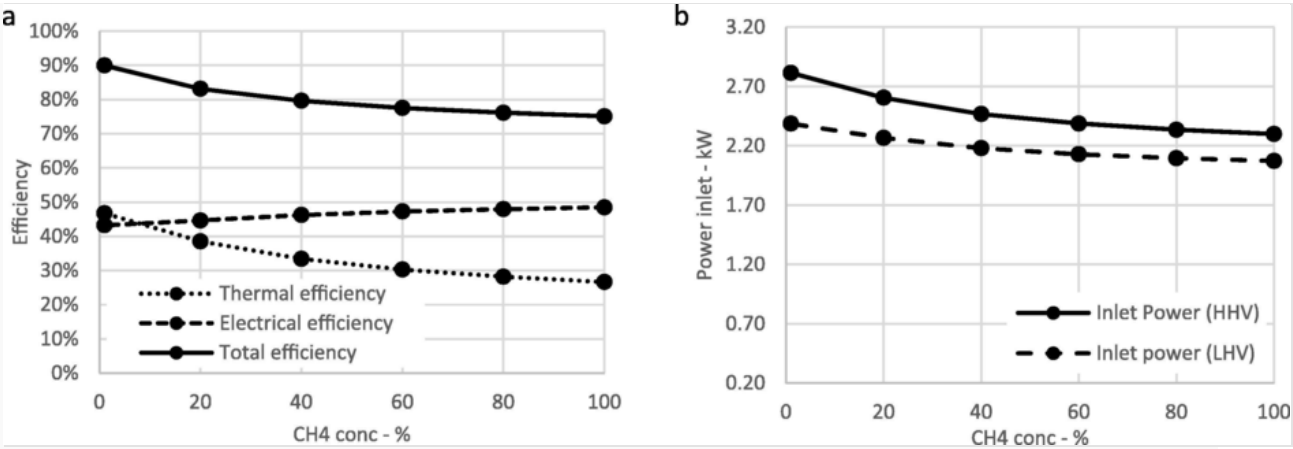

Fig. 5 (a) System electric, thermal and total efficiency and (b) Inlet Power HHV and LHV as a function of Hythane composition.

This trend is partially balanced by the auxiliary power consumption. Figure shows this contribution using two parameters: (a) utilization of oxygen – U_{ox} (Figure a), and (b) the auxiliary power rate itself calculated as the ratio between auxiliary energy consumption and net electrical power output (Figure b). As previously commented, the introduction of hydrogen into the system leads to an increase of stack performance, less thermal losses in the stack and consequently a lower air flow being the main gas flow cooling the fuel cell. A lower air flow obviously results in a higher U_{ox} and a lower amount of auxiliary power needed for the air blower as shown in Fig. 6a and b. (Note that a higher hydrogen concentration is to be found at the left hand side of the X-axis).

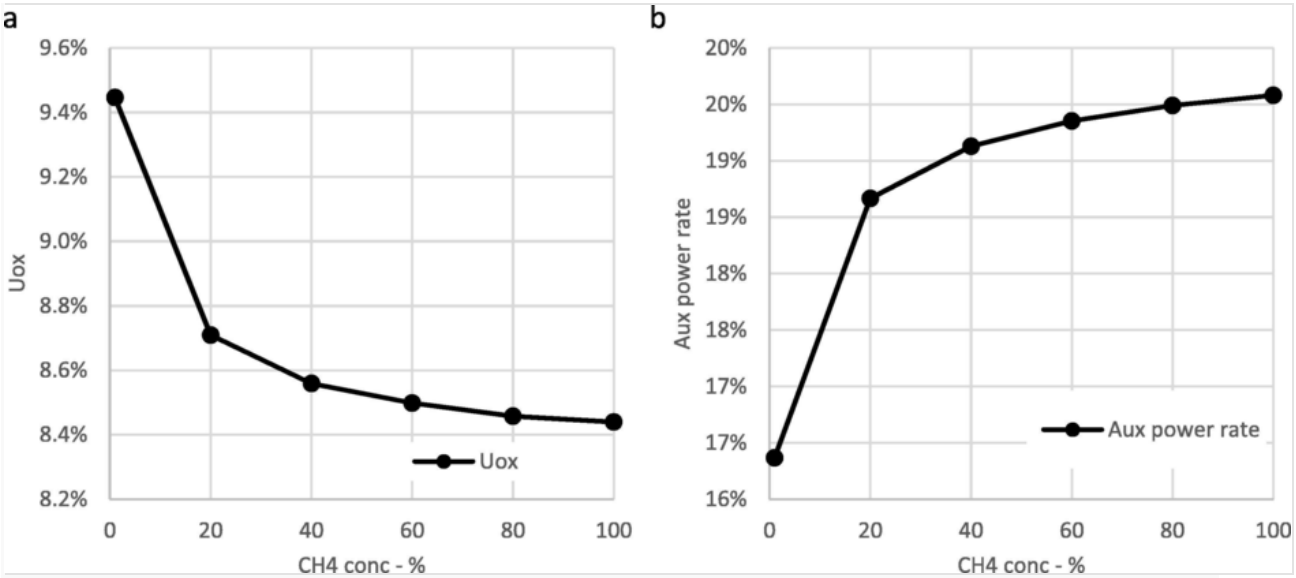

Fig. 6 (a) Uox and (b) auxiliary power rate as a function of Hythane composition.

3.2 Internal reforming

In this section we will present and discuss the main results of our simulations on the internal reformer SOFC cogeneration system. In Figs. 7 and 8 cell voltage, current density and stack and system efficiencies are depicted and compared with the results presented above for the external reforming system. Fig. 7a reports voltage and current values as function of Hythane concentration. The internal reforming configuration always shows a better performance compared to external reforming. Fig. 7b shows that maximum stack efficiency is obtained for pure methane with a difference in stack efficiency of more than 10 percent points between external and internal reforming. This result is mainly related to the higher cell voltage of the direct internal reforming stack as shown in Fig. 7a.

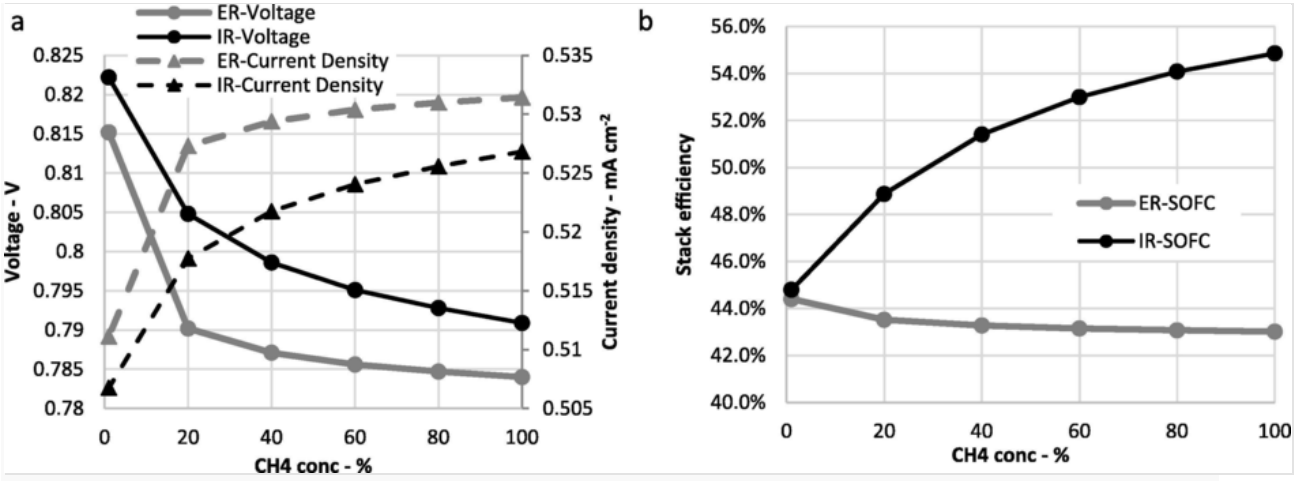

Fig. 7 A comparison of Stack performances of internal and external reforming configurations in terms of (a) voltage and current and (b) in terms of efficiency as a function of Hythane composition.

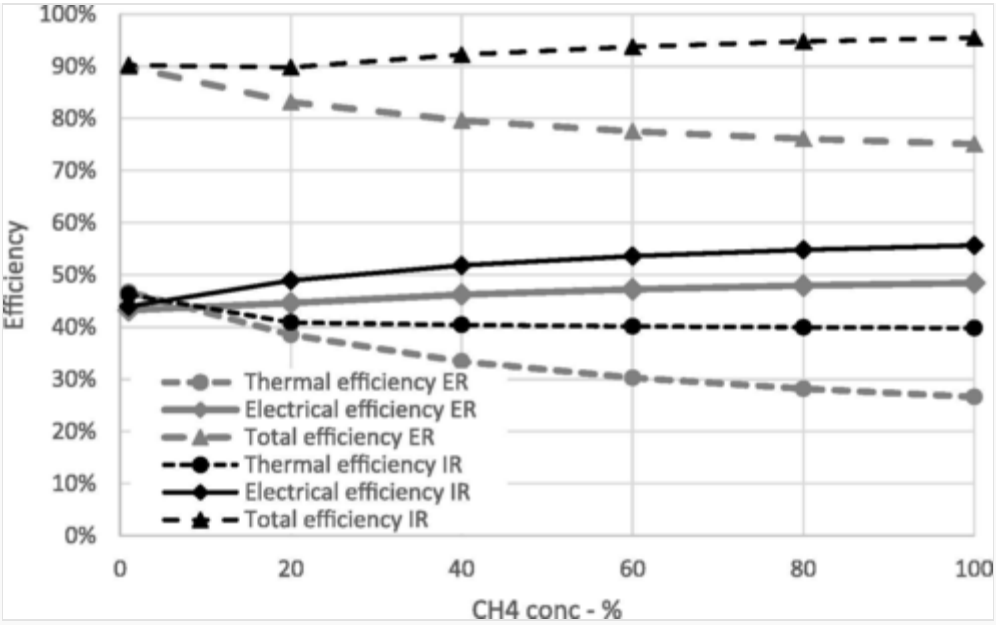

Fig. 8 System efficiencies of internal (IR) and external (ER) reforming configurations compared. as a function of Hythane composition.

System efficiencies are reported in Fig. 8. The internal reforming configuration brings several advantages in terms of electrical efficiency due to improved stack performance and reduced auxiliary power consumed in the blower. The air flow needed to cool down the stack can be lower thanks to the endothermic internal reforming reactions. Nevertheless, thermal efficiency is higher due to the higher temperature of the off gasses. Fig. 9 reports oxidant utilization U_{ox} and auxiliary power rate as a function of CH_4 concentration for the internal reforming configuration. Both graphs have opposite trends compared to the ER configuration. Oxidant utilization U_{ox} increases almost linearly with increasing methane concentration. Again, the increase is due to the endothermic reforming reaction that reduces the need for coolant and consequently power consumption by the air blower, the main constituent of the auxiliary power rate, also decreases with increased methane concentration in the fuel blend.

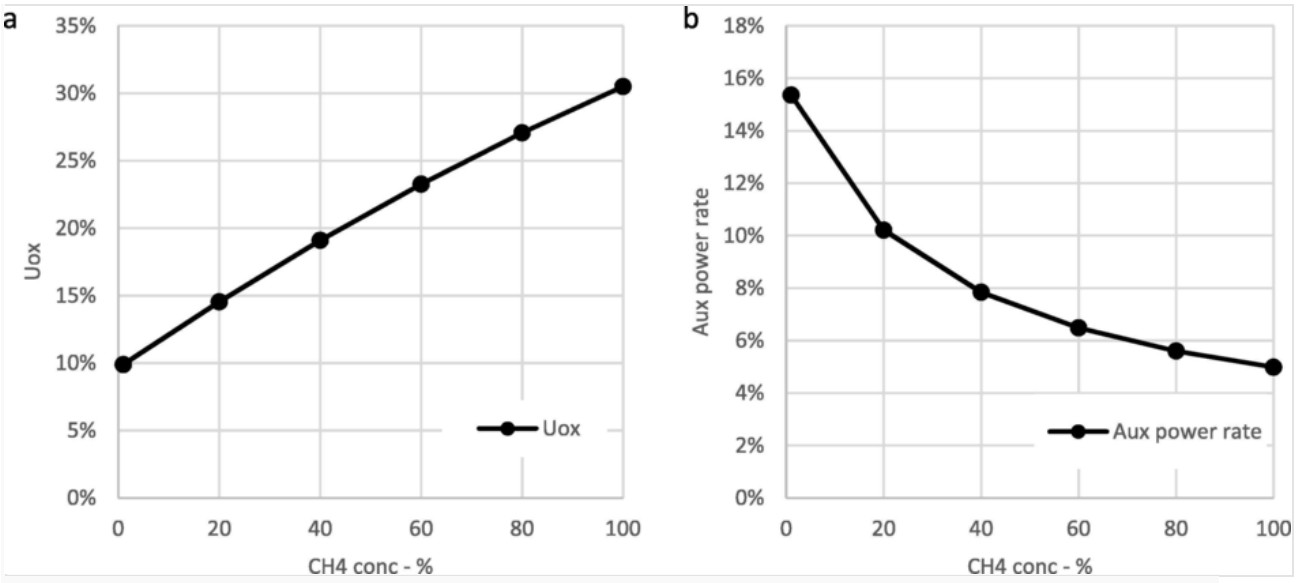

Fig. 9 (a) U_{ox} and (b) auxiliary power rate of IR SOFC system as a function of Hythane composition.

As already stated, system efficiencies depend on the percentage of hydrogen in the natural gas grid used to fuel the system. Then it is better possible to decide how to operate the system, depending mainly on (time dependent) demand for power and heat and their time dependent market prices in order to achieve the economic optimum operating conditions. A useful parameter, typical of cogeneration analysis, is the Electric Index (EI), defined as the ratio between the amount of electrical power and thermal power produced. As an example, Fig. 10 reports the Electric Index of the system with external reforming. In the figure and arrow indicates the direction in which CH_4 concentration increases; a higher CH_4 concentration gives a lower total efficiency. The plot shows that when total efficiency increases (for decreasing CH_4 concentration) a decrease of the Electric index is found. This is accompanied by a higher production of heat from the CHP system.

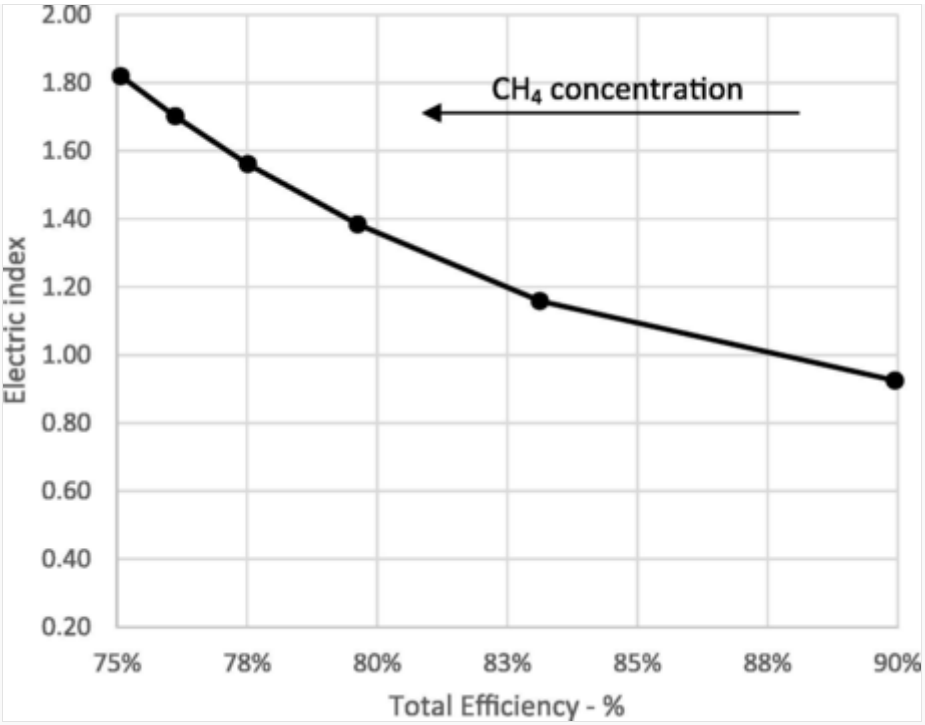

Fig. 10 Electric Index as function of total efficiency.

4 Discussion.

We emphasize that a transition of natural gas (methane) to a mixture of methane and hydrogen has consequences for applications based on combustion where possibly gas burners need to be replaced. (Such a huge substitution of burners in gas stoves and furnaces in individual homes has already once taken place namely in the Netherlands in the early 60-ies of last century, when the largest natural gas field of Europe was found in the province of Groningen. However, also for (future) systems based on (high temperature) fuel cells such as SOFC's in CHP applications. A change of fuel from methane or hydrogen to a mixture of both can have consequences for the operation and performance of such combined heat and power systems.

In future scenario's where CHP will be deployed at a local (household) level systems fed by the natural gas grid, as well as units operating on stored hydrogen may be envisaged. As we have shown in this study that SOFC based μCHP units can operate on both fuels; hydrogen and methane and all mixture thereof. This allows for efficient and convenient hydrogen integration strategies in an energy transition to lower carbon fuels in order to reduce CO_2 emissions while using in principle, the same SOFC CHP unit. However, our study also shows that a possible future switch from natural gas to Hythane will have consequences for the operation and performance of such μCHP systems. Surprisingly, electrical efficiency decreases with an increase in hydrogen content while, on the other hand, thermal efficiency and total efficiency increases. Moreover, the use of Hythane allows for the use of an internal reforming SOFC with additional advantages in terms of increased thermal and electrical efficiency with respect to external reforming and relaxed design and operating conditions with respect to the prevention of temperature gradients and shocks in de SOFC stack

as would normally occur with the use of pure methane due to its fast reforming reaction and the endothermic nature of this reaction. The presence of hydrogen in the fuel mixture at the inlet prevents the presence of a strong heat sink at the inlet side of the stack.

The practical consequences for the operation of such systems in the future can be found in the detailed design modification next to the modified operation of these systems that might be necessary in particular if the composition of the fuel may vary in time during operation of the CHP unit. Moreover, a recalculation of the economic return on investment would be necessary since a shift from electricity to heat production occurs for increasing hydrogen content in the Hythane fuel blend.

5 Conclusions

This study evaluates the performance of a SOFC based μCHP system in a future scenario where the system is fed with Hythane: a mixture of methane and hydrogen. We have shown that the use of Hythane compared to pure methane increases total efficiency in terms of power plus heat of a SOFC combined heat and power system, yet at the expense of a decrease in electric efficiency with a few point percent. When one accounts for these changes in efficiency the SOFC based cogeneration systems are suitable for operation in an energy system in transition from natural gas to Hythane and pure hydrogen. Internal reforming systems show higher thermal, electric and overall efficiencies and are very suitable for operation with Hythane since those gas compositions reduce internal temperature gradients in the IR-SOFC stack compared to operation on methane and pre-reformers may no longer be needed in those system designs.

References

[1] L. van de Beld, I. Bouwmans, P.A.M. Claassen, K. Hemmes, H. de Wit, N. Woudstra, et al., Exploring new production methods of hydrogen/natural gas blends for mixing into the natural gas network of the Netherlands, ECOS 2003; 16th Int. Conf. Effic. Costs, Optim. Simul. Environ. Impact Energy Syst. Copenhagen, Denmark (30-06 to 02-07-2003), Copenhagen, 2003.

[2] O. Florisson, NATURALHY: assessing the potential of the existing natural gas network for hydrogen delivery, GERG Acad Netw Event, 4 June 2010, Brussles, Belgium, 2010.

[3] K. Altfeld and D. Pinchbeck, Admissible hydrogen concentrations in natural gas systems, *Gas Energy* 2013, 1–16, doi:ISSN 2192-158X.

[4] H. de Vries, A.V. Mokhov and H.B. Levinsky, The impact of natural gas/hydrogen mixtures on the performance of end-use equipment: Interchangeability analysis for domestic appliances, *Appl Energy* **208**, 2017, 1007–1019, https://doi.org/10.1016/J.APENERGY.2017.09.049.

[5] G. Guandalini, P. Colbertaldo and S. Campanari, Dynamic modeling of natural gas quality within transport pipelines in presence of hydrogen injections, *Appl Energy* **185**, 2017, 1712–1723, https://doi.org/10.1016/J.APENERGY.2016.03.006.

[6] M. Abeysekera, J. Wu, N. Jenkins and M. Rees, Steady state analysis of gas networks with distributed injection of alternative gas, *Appl Energy* **164**, 2016, 991–1002, https://doi.org/10.1016/J.APENERGY.2015.05.099.

[7] M. Talibi and R. Balachandran, Ladommatos N. Influence of combusting methane-hydrogen mixtures on compression–ignition engine exhaust emissions and in-cylinder gas composition, *Int J Hydrogen Energy* 2016, 1–16, https://doi.org/10.1016/j.ijhydene.2016.10.049, Article.

[8] Battistoni M, Poggiani C, Grimaldi CN. Experimental investigation of a port fuel injected spark ignition engine fuelled with variable mixtures of hydrogen and methane; 2013. http://doi.org/10.4271/2013-01-0226.

[9] E. Navarro, T.J. Leo and R. Corral, CO_2 emissions from a spark ignition engine operating on natural gas–hydrogen blends (HCNG), *Appl Energy* **101**, 2013, 112–120, https://doi.org/10.1016/J.APENERGY.2012.02.046.

[10] A.K. Sen, J. Wang and Z. Huang, Investigating the effect of hydrogen addition on cyclic variability in a natural gas spark ignition engine: wavelet multiresolution analysis, *Appl Energy* **88**, 2011, 4860–4866, https://doi.org/10.1016/J.APENERGY.2011.06.030.

[11] R. O'Shea, D. Wall, I. Kilgallon and J.D. Murphy, Assessment of the impact of incentives and of scale on the build order and location of biomethane facilities and the feedstock they utilise, *Appl Energy* **182**, 2016, 394–408, https://doi.org/10.1016/J.APENERGY.2016.08.063.

[12] R. O'Shea, D.M. Wall, I. Kilgallon, J.D. Browne and J.D. Murphy, Assessing the total theoretical, and financially viable, resource of biomethane for injection to a natural gas network in a region, *Appl Energy* **188**, 2017, 237–256, https://doi.org/10.1016/J.APENERGY.2016.11.121.

[13] T. Horschig, P.W.R. Adams, E. Gawel and D. Thrän, How to decarbonize the natural gas sector: a dynamic simulation approach for the market development estimation of renewable gas in Germany, *Appl Energy* **213**, 2018, 555–572, https://doi.org/10.1016/J.APENERGY.2017.11.016.

[14] F. Cucchiella, I. D'Adamo, M. Gastaldi and M. Miliacca, A profitability analysis of small-scale plants for biomethane injection into the gas grid, *J Clean Prod* **184**, 2018, 179–187, https://doi.org/10.1016/J.JCLEPRO.2018.02.243.

[15] G. Li, R. Zhang, T. Jiang, H. Chen, L. Bai and X. Li, Security-constrained bi-level economic dispatch model for integrated natural gas and electricity systems considering wind power and power-to-gas process, *Appl Energy* **194**, 2017, 696–704, https://doi.org/10.1016/J.APENERGY.2016.07.077.

[16] M. Bailera, S. Espatolero, P. Lisbona and L.M. Romeo, Power to gas-electrochemical industry hybrid systems: a case study, *Appl Energy* **202**, 2017, 435–446, https://doi.org/10.1016/J.APENERGY.2017.05.177.

[17] E. Frank, J. Gorre, F. Ruoss and M.J. Friedl, Calculation and analysis of efficiencies and annual performances of Power-to-Gas systems, *Appl Energy* **218**, 2018, 217–231, https://doi.org/10.1016/J.APENERGY.2018.02.105.

[18] Z. Huang, L. Lu, D. Jiang, D. Xing and Z.J. Ren, Electrochemical Hythane production for renewable energy storage and biogas upgrading, *Appl Energy* **187**, 2017, 595–600, https://doi.org/10.1016/J.APENERGY.2016.11.099.

[19] R. Judd and D. Pinchbeck, Hydrogen admixture to the natural gas grid, In: *Compend. Hydrog. Energy*, 2016, Elsevier, 165–192, https://doi.org/10.1016/B978-1-78242-364-5.00008-7.

[20] S. Schiebahn, T. Grube, M. Robinius, V. Tietze, B. Kumar and D. Stolten, Power to gas: Technological overview, systems analysis and economic assessment for a case study in Germany, *Int J Hydrogen Energy* **40**, 2015, 4285–4294, https://doi.org/10.1016/J.IJHYDENE.2015.01.123.

[21] G. Cinti and K. Hemmes, Integration of direct carbon fuel cells with concentrated solar power, *Int J Hydrogen Energy* **36**, 2011, 10198–10208, https://doi.org/10.1016/j.ijhydene.2010.11.019.

[22] J. Guerrero, F. Blaabjerg, T. Zhelev, K. Hemmes, E. Monmasson, S. Jemei, et al., Distributed Generation: Toward a New Energy Paradigm, *IEEE Ind Electron Mag* **4**, 2010, 52–64, https://doi.org/10.1109/MIE.2010.935862.

[23] V. Verda and M. Caliquaglia, Solid oxide fuel cell systems for distributed power generation and cogeneration, *Int J Hydrogen Energy* **33**, 2008, 2087–2096, https://doi.org/10.1016/j.ijhydene.2008.01.046.

[24] Elcogen, Convion supply SOFC CHP systems to business district smart grid project in Finland, *Fuel Cells Bull* **2018**, 2018, 1, https://doi.org/10.1016/S1464-2859(18)30034-8.

[25] Callux residential demonstrations reach 1m hours of operation. Fuel Cells Bull 2012;2012:5–6. http://doi.org/10.1016/S1464-2859(12)70162-1.

[26] European ene.field project highlights fuel cell micro-cogeneration. Fuel Cells Bull 2017;2017:6–7. http://doi.org/10.1016/S1464-2859(17)30382-6.

[27] M. Kadowaki, Current status of national SOFC projects in Japan, *ECS Trans* **68**, 2015, 15–22, https://doi.org/10.1149/06801.0015ecst.

[28] H. Ito, Economic and environmental assessment of residential micro combined heat and power system application in Japan, *Int J Hydrogen Energy* **41**, 2016, 15111–15123, https://doi.org/10.1016/j.ijhydene.2016.06.099.

[29] M. Andersson, H. Nakajima, T. Kitahara, A. Shimizu, T. Koshiyama, H. Paradis, et al., Comparison of humidified hydrogen and partly pre-reformed natural gas as fuel for solid oxide fuel cells applying computational fluid dynamics, *Int J Heat Mass Transf* **77**, 2014, 1008–1022, https://doi.org/10.1016/j.ijheatmasstransfer.2014.06.033.

[30] V. Liso, M.P. Nielsen and S.K. Kær, Influence of anodic gas recirculation on solid oxide fuel cells in a micro combined heat and power system, *Sustain Energy Technol Assessments* **8**, 2014, 99–108, https://doi.org/10.1016/j.seta.2014.08.002.

[31] V. Liso, A.C. Olesen, M.P. Nielsen and S.K. Kær, Performance comparison between partial oxidation and methane steam reforming processes for solid oxide fuel cell (SOFC) micro combined heat and power (CHP) system, *Energy* **36**, 2011, 4216–4226, https://doi.org/10.1016/j.energy.2011.04.022.

[32] T. Pfeifer, L. Nousch, D. Lieftink and S. Modena, System design and process layout for a SOFC micro-CHP unit with reduced operating temperatures, *Int J Hydrogen Energy* **38**, 2013, 431–439, https://doi.org/10.1016/J.IJHYDENE.2012.09.118.

[33] C. Ni, Z. Yuan, S. Wang, D. Li, C. Zhang, J. Li, et al., Study on an integrated natural gas fuel processor for 2-kW solid oxide fuel cell, *Int J Hydrogen Energy* **40**, 2015, 15491–15502, https://doi.org/10.1016/j.ijhydene.2015.09.067.

[34] T. Kushi, Heat balance of dry reforming in solid oxide fuel cell systems, *Int J Hydrogen Energy* **42**, 2017, 11779–11787, https://doi.org/10.1016/j.ijhydene.2017.02.112.

[35] L. Barelli, G. Bidini, G. Cinti, F. Gallorini and M. Pöniz, SOFC stack coupled with dry reforming, *Appl Energy* **192**, 2017, 498–507, https://doi.org/10.1016/j.apenergy.2016.08.167.

[36] V. Liso, Y. Zhao, N.P. Brandon, M.P. Nielsen and S.K. Kær, Analysis of the impact of heat-to-power ratio for a SOFC-based mCHP system for residential application under different climate regions in Europe, *Int J Hydrogen Energy* **36**, 2011, 13715–13726, https://doi.org/10.1016/j.ijhydene.2011.07.086.

[37] E.J. Naimaster and A.K. Sleiti, Potential of SOFC CHP systems for energy-efficient commercial buildings, *Energy Build* **61**, 2013, 153–160, https://doi.org/10.1016/j.enbuild.2012.09.045.

[38] A. Adam, E.S. Fraga and D.J.L. Brett, Options for residential building services design using fuel cell based micro-CHP and the potential for heat integration, *Appl Energy* **138**, 2015, 685–694, https://doi.org/10.1016/J.APENERGY.2014.11.005.

[39] T.C. Fubara, F. Cecelja and A. Yang, Modelling and selection of micro-CHP systems for domestic energy supply: the dimension of network-wide primary energy consumption, *Appl Energy* **114**, 2014, 327–334, https://doi.org/10.1016/J.APENERGY.2013.09.069.

[40] S. Giarola, O. Forte, A. Lanzini, M. Gandiglio, M. Santarelli and A. Hawkes, Techno-economic assessment of biogas-fed solid oxide fuel cell combined heat and power system at industrial scale, *Appl Energy* **211**, 2018, 689–704, https://doi.org/10.1016/j.apenergy.2017.11.029.

[41] A. Thallam Thattai, V. Oldenbroek, L. Schoenmakers, T. Woudstra and P.V. Aravind, Experimental model validation and thermodynamic assessment on high percentage (up to 70%) biomass co-gasification at the 253 MWe integrated gasification combined cycle power plant in Buggenum, The Netherlands, *Appl Energy* **168**, 2016, 381–393, https://doi.org/10.1016/J.APENERGY.2016.01.131.

[42] H.-K. Seo, W. Park and H.C. Lim, The efficiencies of internal reforming molten carbonate fuel cell fueled by natural gas and synthetic natural gas from coal, *J Electrochem Energy Convers Storage* **13**, 2016, , 011005https://doi.org/10.1115/1.4033255.

[43] H. Ghadamian, A.A. Hamidi, H. Farzaneh and H.A. Ozgoli, Thermo-economic analysis of absorption air cooling system for pressurized solid oxide fuel cell/gas turbine cycle, *J Renew Sustain Energy* **4**, 2012, 43115, https://doi.org/10.1063/1.4742336.

[44] http://www.asimptote.nl/software/cycle-tempo/cycle-tempo-model-examples/

[45] SOLIDPower. ASC-700 Datasheet

[46] FCH2 JU. Multi – Annual Work Plan 2014 – 2020; 2014.